Available online at www.sciencedirect.com
SCIENCE DIRECT
Journal of Organometallic Chemistry 691 (2006) 2767–2773
Journal of Organometallic Chemistry
www.elsevier.com/locate/jorganchem

Color tuning of iridium complexes for organic light-emitting diodes: The electronegative effect and π-conjugation effect

Cheng-Hsien Yang, Kai-Hung Fang, Wei-Lin Su, Shao-Pin Wang, Shih-Kang Su, I-Wen Sun *

Department of Chemistry, National Cheng Kung University, Tainan, Taiwan, 701, Republic of China

Received 4 January 2006; received in revised form 3 February 2006; accepted 9 February 2006
Available online 3 March 2006

Abstract

Novel red phosphorescent emitter bis(4-phenylquinazolinato-N,$C^{2'}$) iridium(acetylacetonate) [$(pqz)_2Ir(acac)$], bis(1-(1′-naphthyl)-5-methylisoquinolinato-N,$C^{2'}$)iridium(acetylacetonate) [$(1\text{-}mniq)_2Ir(acac)$] and bis(1-(2′-naphthyl)-5-methylisoquinolinato-N,$C^{2'}$)iridium(acetylacetonate) [$(2\text{-}mniq)_2Ir(acac)$] have been synthesized and fully characterized. The electronegative effect of $(pqz)_2Ir(acac)$ ligand shows almost the same influence as the extended π-conjugation effect of $(2\text{-}mniq)_2Ir(acac)$. Density functional theory (DFT) was applied to calculate the Kohn–Sham orbitals of HOMOs and LUMOs in the iridium complexes to illustrate the N(1) electronegative atom effect. Finally, lowest triplet state (T_1) energies calculated by time-dependent DFT (TDDFT) were compared with the experimental electroluminescent data. The calculated data for the iridium complexes agreed fairly well with experimental data. Electroluminescent devices with a configuration of ITO/NPB/CBP:dopant/BCP/AlQ_3/LiF/Al were fabricated. The device using $(pqz)_2Ir(acac)$ as a dopant showed deep-red emission with 1931 CIE (Commission International de L'Eclairage) chromaticity coordinates $x = 0.70$, $y = 0.30$.

Keywords: Iridium; Red emitter; Organic light-emitting diodes

1. Introduction

Organic light-emitting diodes (OLEDs) are one of the most important low cost full-color flat panel display alternatives to liquid crystal displays. Since the red-emitting phosphorescent dopants have been reported, OLEDs have made great progress and received considerable attention [1–5]. High-efficiency red emission could be anticipated for display applications by carefully designing appropriate ligands to form light-emitting iridium complexes [6,7]. Okada et al. [8] demonstrated a high efficiency red OLED using $Ir(piq)_3$ [iridium(III) tris(1-phenylisoquinolinato-N,$C^{2'}$)] as the dopant, which exhibited a maximum emission peak at 623 nm. The efficiency of the electroluminescence device was 8.0 lm/W, 9.3 cd/A at 100 cd/m^2 and 6.3 lm/W, 8.4 cd/A at 300 cd/m^2, and the CIE (Commission International de L'Eclairage) coordinate was (0.68, 0.33). Photophysical properties can be affected by extending the π-conjugation system of the ligand. Recently, by modifying the ligands, we have successfully shifted the red emission from 624 nm to 680 nm [9].

Quinazoline alkaloid can be found in *Dichroa febriguga* Lour., it contains antimalarial constituents and has been used in Chinese medicine [10]. Although quinazoline derivatives abound in the nature, investigations focused on using quinazoline as a ligand for iridium complex for OLEDs are very limited. Because of the similarity in the structures of 1-phenylisoquinoline and 4-phenylquinazoline, it is interesting to study the effect of the N(1) electronegative atom of the 4-phenylquinazoline on the properties of its iridium complex. In this paper, we compared the

* Corresponding author. Tel.: +886 6275 7575x65355; fax: +886 6274 0552.
E-mail address: iwsun@mail.ncku.edu.tw (I-Wen Sun).

0022-328X/$ - see front matter © 2006 Elsevier B.V. All rights reserved.
doi:10.1016/j.jorganchem.2006.02.034

4-phenylquinazoline ligand to a series of phenyl-methylisoquinoline ligands and applied the density functional theory (DFT) to calculate the Kohn–Sham orbitals of highest occupied molecular orbital (HOMO) and lowest unoccupied molecular orbital (LUMO) for these complexes, and lowest triplet state (T_1) energies calculated by time-dependent DFT in order to get a better understanding on the N(1) electronegative effect.

2. Experimental

^{1}H NMR and ^{13}C NMR spectra were measured in CD_2Cl_2 solution on Bruker Avance-300 (300 MHz) or AMX-400 (400 MHz) NMR spectrometers with tetramethylsilane (TMS) as the internal standard. The EI-Mass spectra were recorded on a Bruker APEX II. The UV–Vis spectra were measured in CH_2Cl_2 solution on an Agilent 8453 spectrophotometer, and the photoluminescence spectra were recorded in CH_2Cl_2 solution with a HITACHI model F-2500 fluorescence spectrophotometer. Melting points were measured using capillary melting point apparatus. HRMS spectra were obtained using a MAT-95XL high-resolution mass spectrometer. Elemental analyses have been carried out by using an Elementar vario EL III analyzer. Phenyl-methylisoquinoline ligands and 4-phenylquinazoline were synthesized using the process reported by Yang [9] and Uff [11], respectively. Cyclometalated Ir(III) μ-chloro-bridged dimers were synthesized by the method reported by Lamansky [4].

2.1. 4-phenylquinazoline (4-pqz)

4-pqz ligand was obtained from the condensation reaction of 2-aminobenzophenone and formamide, according to the literature method [11]. $T_m = 95.0$–97.0 °C; EIMS: m/z 206, $[M]^+$; HREIMS calcd for $C_{14}H_{10}N_2$, 206.0844, found 206.0843. ^{1}H NMR ($CDCl_3$, 300 MHz): δ 9.39 (s, 1H), 8.13–8.16 (m, 2H), 7.93 (t, $J = 7.7$ Hz, 1H), 7.78–7.79 (m, 2H), 7.65–7.57 (m, 4H). ^{13}C NMR ($CDCl_3$, 100 MHz) δ: 168.6, 154.3, 150.7, 136.9, 133.9, 130.2, 130.0, 128.6, 127.9, 127.1, 123.1.

2.2. 1-(1′-naphthyl)-5-methylisoquinoline (1-mniq)

1-mniq ligand was prepared by a modified method [9]. First, naphthalene-1-carboxylic acid phenethyl-amide was synthesized and introduced with a cyclization process to obtain 1-naphthalen-1-yl-3,4-dihydro-isoquinoline. After deprotonation of this, the white solid product was obtained in a 38.7% yield. $T_m = 140.9$–141.7 °C; EIMS: m/z 269, $[M]^+$; HREIMS calcd for $C_{20}H_{15}N$, 269.1204, found 269.1206. ^{1}H NMR ($CDCl_3$, 300 MHz): δ 8.72 (d, $J = 5.9$ Hz, 1H), 7.99–7.87 (m, 3H), 7.63–7.44 (m, 5H), 7.37–7.24 (m, 3H), 2.75 (s, 3H). ^{13}C NMR ($CDCl_3$, 100 MHz) δ: 137.2, 135.9, 133.7, 133.6, 132.3, 130.6, 128.7, 128.3, 128.2, 127.6, 126.7, 126.2, 126.0, 125.9, 125.8, 125.1, 18.9.

2.3. 1-(2′-naphthyl)-5-methyl isoquinoline (2-mniq)

2-mniq ligand was prepared as described in 1-mniq, and the white solid product was obtained in a 19.6% yield. $T_m = 115.8$–117.0 °C; EIMS: m/z 269, $[M]^+$; HREIMS calcd for $C_{20}H_{15}N$, 269.1204, found 269.1204. ^{1}H NMR ($CDCl_3$, 300 MHz): δ 8.69 (d, $J = 5.9$ Hz, 1H), 8.17 (s, 1H), 8.01–7.81 (m, 6H), 7.58–7.53 (m, 3H), 7.42 (t, $J = 7.4$ Hz, 1H), 2.74 (s, 3H). ^{13}C NMR ($CDCl_3$, 100 MHz) δ: 141.9, 137.1, 136.4, 133.9, 133.2, 133.1, 130.5, 129.5, 128.5, 128.0, 127.7, 127.6, 126.9, 126.8, 126.5, 126.3, 125.8, 19.0.

2.4. Bis(4-phenylquinazolinato-N,C$^{2'}$)-iridium(acetylacetonate), (4-pqz)$_2$Ir(acac)

(4-pqz)$_2$Ir(acac) was dried and column chromatography was used to give red solid product in a 63.5% yield. EIMS: m/z 702, $[M]^+$; HREIMS calcd for $C_{33}H_{25}IrO_2N_4$, 702.1607, found 702.1613. ^{1}H NMR (CD_2Cl_2, 300 MHz): δ 9.14 (s, 2H), 8.93 (d, $J = 8.5$ Hz, 2H), 8.40 (d, $J = 7.7$ Hz, 2H), 8.17 (d, $J = 8.5$ Hz, 2H), 7.95 (t, $J = 7.8$ Hz, 2H), 7.82 (t, $J = 8.0$ Hz, 2H), 7.02 (t, $J = 7.7$ Hz, 1H), 6.76 (t, $J = 7.6$ Hz, 2H), 6.51 (d, $J = 7.7$ Hz, 2H), 5.35 (s, 1H), 1.80 (s, 6H). ^{13}C NMR ($CDCl_3$, 100 MHz) δ: 175.7, 165.3, 146.2, 142.7, 141.4, 134.7, 124.6, 122.3, 121.1, 119.1, 118.5, 116.3, 111.9, 111.4, 91.3, 18.3. Anal. Calc. for $C_{33}H_{25}O_2N_4Ir$: C, 56.48; H, 3.59; N, 7.98. Found: C, 56.11; H, 3.73; N, 7.75%.

2.5. Bis(1-(1′-naphthyl)-5-methylisoquinolinato-N,C$^{2'}$)-iridium(acetylacetonate), (1-mniq)$_2$Ir(acac)

Dark red solid. Yield: 56.8%; EIMS: m/z 828, $[M]^+$; HREIMS calcd for $C_{45}H_{35}IrO_2N_2$, 828.2328, found 828.2330. ^{1}H NMR (CD_2Cl_2, 300 MHz): δ 8.37–8.45 (m, 2H), 8.04 (d, $J = 8.6$ Hz, 2H), 7.74–7.79 (m, 4H), 7.50–7.55 (m, 4H), 7.32–7.37 (m, 2H), 7.02–7.18 (m, 6H), 6.92–7.00 (m, 2H), 2.76 (s, 6H), 1.82 (s, 6H). ^{13}C NMR ($CDCl_3$, 100 MHz) δ: 175.3, 161.4, 146.9, 130.3, 127.0, 123.7, 121.9, 119.2, 118.9, 118.5, 117.8, 115.7, 114.6, 114.5, 112.7, 106.7, 90.9, 18.6, 9.3. Anal. Calc. for $C_{45}H_{35}O_2N_2Ir$: C, 65.28; H, 4.26; N, 3.38. Found: C, 65.15; H, 4.52; N, 3.19%.

2.6. Bis(1-(2′-naphthyl)-5-methylisoquinolin ato-N,C$^{2'}$)-iridium(acetylacetonate), (2-mniq)$_2$Ir(acac)

Red solid. Yield: 62.6%; EIMS: m/z 828, $[M]^+$; HREIMS calcd for $C_{45}H_{35}IrO_2N_2$, 828.2328, found 828.2330. ^{1}H NMR (CD_2Cl_2, 300 MHz): δ 8.96 (d, $J = 8.0$ Hz, 2H), 8.62 (s, 2H), 8.53 (d, $J = 6.7$ Hz, 2H), 7.72 (d, $J = 6.7$ Hz, 2H), 7.60–7.68 (m, 6H), 7.06–7.08 (m, 6H), 6.61 (s, 2H), 5.32 (s, 1H), 2.70 (s, 6H), 1.70 (s, 6H). ^{13}C NMR ($CDCl_3$, 100 MHz) δ: 158.5, 136.1, 133.7, 130.1, 126.4, 124.3, 124.2, 121.7, 120.1, 119.2, 118.0, 117.8, 116.8, 115.4, 115.3, 113.1, 106.8, 90.1, 19.5, 9.3. Anal.

Calc. for $C_{45}H_{35}O_2N_2Ir$: C, 65.28; H, 4.26; N, 3.38. Found: C, 65.16; H, 4.50; N, 3.24%.

3. Computational methodology

The ground state geometries for these four complexes were optimized by density functional theory (DFT) level of calculation with B3LYP [12,13] functional employing Gaussian 98 [14] software package. Double-ζ quality plus polarization function basis sets were employed for all of the ligands (6-31G*) and the Ir (LANL2DZ). A relativistic effective core potential (ECP) [15] on Ir replace the inner core electrons leaving the outer core $[(5s)^2(5p)^6]$ electrons and the $(5d)^6$ valence electrons of Ir(III). Although the geometries were fully optimized without any symmetry constraints, the symmetries of theses complexes are very closed to C_2 point group.

Time-dependent density functional theory (TDDFT) [16–18] calculations were also performed with B3LYP functional at the same basis sets level under optimized ground state geometries to get excited state energies, which give a vertical excitation (Frank–Condon principle) approach that could be comparable to experimental data of emission. TDDFT allowed the computation of excited state energies, oscillator strengths, and the excited state compositions in term of excitation between occupied and virtual molecular orbitals. It is informative that TDDFT provides correlation between molecular orbitals and excited states. Similar applications of TDDFT have been used to investigate the properties of cyclometalated iridium (III) compounds [19,20].

4. Results and discussion

Phenyl-methylisoquinoline ligands and 4-phenylquinazoline were synthesized using the process reported by Yang [9] and Uff [11], respectively. We prepared 1-phenyl-5-methylisoquinoline (m-piq), 1-(1′-naphthyl)-5-methylisoquinoline (1-mniq), 1-(2′-naphthyl)-5-methyl isoquinoline (2-mniq) and 4-phenylquinazoline (4-pqz), and compared the properties of the corresponding iridium complexes using $(m\text{-}piq)_2Ir(acac)$ as the reference material. As shown in Scheme 1, all ligands were reacted with iridium trichloride to form dimers, $[(C\hat{}N)_2Ir(\mu\text{-}Cl)_2Ir(C\hat{}N)_2]$, followed by the reaction with acetylacetone in the presence of sodium carbonate [4]. All procedures involving Ir(III) species were carried out under nitrogen gas atmosphere despite the air stability of the complexes. All of these materials were characterized by ^1H, ^{13}C NMR, mass spectrometry and elemental analyses.

The absorption and photoluminescence (PL) spectra of the iridium compounds in CH_2Cl_2 are shown in Fig. 1. The strong absorption peaks between 230 and 360 nm can be assigned to the spin-allowed $^1\pi$–π^* transition of the cyclometalated ligand. Due to the perturbation from iridium metal, these transitions have shifted with respect to that of the free ligand. The band around 450 nm can be assigned to the spin-allowed metal–ligand charge transfer band (^{1}MLCT) and the shoulder around 500 nm can be assigned to the spin-forbidden ^{3}MLCT band [21]. These bands are not observed for the free ligand precursors.

As shown in Fig. 1, while the PL spectrum of the reference material, $(m\text{-}piq)_2Ir(acac)$, in CH_2Cl_2 shows an emission band at 623.5 nm, the other complexes $(2\text{-}mniq)_2Ir(acac)$,

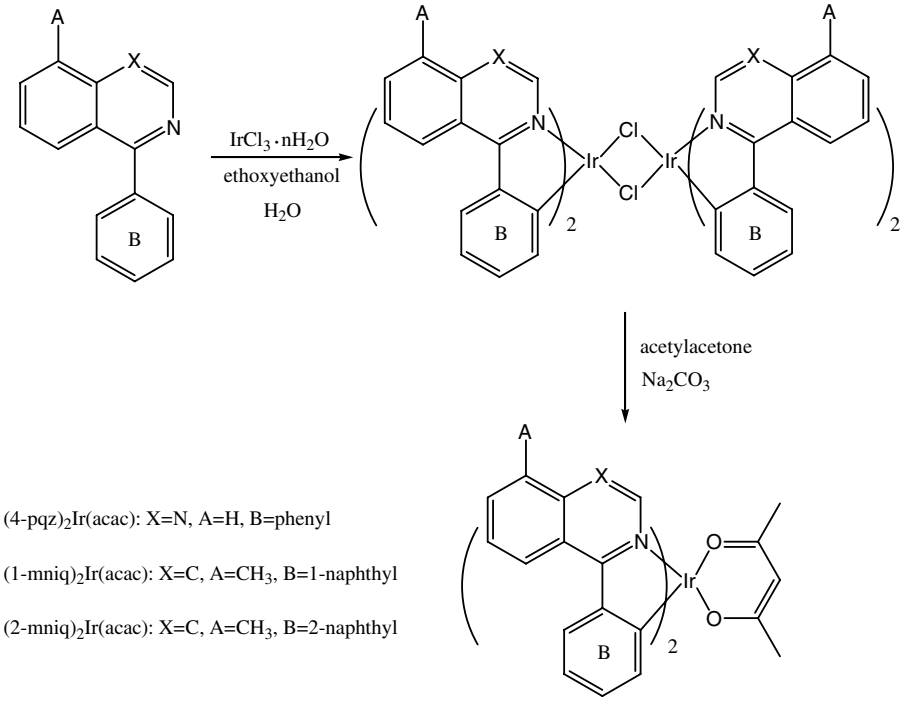

Scheme 1. Synthesis of iridium complexes.

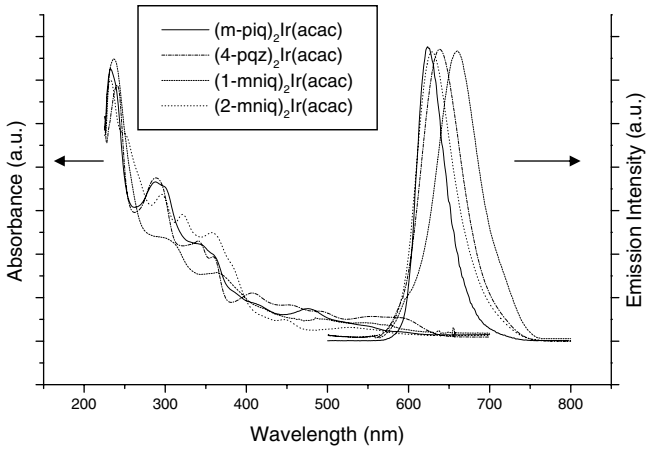

Fig. 1. Absorption and photoluminescence spectra of iridium complexes in CH_2Cl_2.

$(4\text{-pqz})_2$Ir(acac) and $(1\text{-mniq})_2$Ir(acac) exhibit bathochromic shift at 629.5, 638.0 and 660.0 nm, respectively. Fig. 2 shows the EL spectra of the devices constructed with these four iridium complexes recorded at a voltage of $V = 7$ V. The EL spectrum of $(\text{m-piq})_2$Ir(acac) shows the red emission band at 622.1 nm, the other complexes $(2\text{-mniq})_2$Ir(acac), $(4\text{-pqz})_2$Ir(acac) and $(1\text{-mniq})_2$Ir(acac) exhibit red shift at 639.0, 650.3 and 669.5 nm, respectively. The EL spectra for these complexes show the same trends as the PL spectra. Interestingly, $(2\text{-mniq})_2$Ir(acac) shows an emission band at 639.0 nm, whereas $(4\text{-pqz})_2$Ir(acac) exhibits a 26 nm red shift to give an emission band at 650.3 nm. This result implies that the N(1) electronegative atom of 4-phenylquinazoline for iridium complex disturbs the electron density of the ligand, resulting in a decrease in the energy band gap of $(4\text{-pqz})_2$Ir(acac) and the bathochromic shift. Although $(4\text{-pqz})_2$Ir(acac) shows more significant red-shift than $(2\text{-mniq})_2$Ir(acac), the devices of these two compounds show almost the same luminance efficiency (vide infra). This result suggests that the N(1) electronegative atom of 4-phenylquinazoline for iridium complex may have facilitated the efficiency of OLEDs.

The HOMO energy of the iridium complexes was estimated by cyclic voltammetry [22]. The voltammograms were recorded at a Pt disk electrode (BAS Co.) in CH_2Cl_2 solutions containing 0.001 M Ir(III)-complex compounds and 0.1 M tetra-*n*-butylammonium perchlorate as the supporting electrolyte. The potential was reported against Ag/$AgNO_3$ (0.01 M in acetonitrile). A typical cyclic voltammogram of the $(4\text{-pqz})_2$Ir(acac) as well as that of ferrocene is shown in Fig. 3 for illustration. All of the iridium complexes synthesized in this study underwent a reversible one-electron oxidation/reduction process. The energy band gap was evaluated from the long-wavelength absorption edge using the theory reported by Burrows et al. [22]. From the oxidation potential data and the absorption-edge data collected from spectroscopic method, values of the HOMO and LUMO of the iridium complexes were calculated [22] and summarized together with the energy gap in Table 1. The values of all the iridium complexes are comparable with the values of $Ir(piq)_3$ that were reported by Okada et al. [8].

Devices were fabricated by high vacuum (10^{-6} Torr) thermal evaporation on pre-cleaned indium-tin-oxide (ITO) glass substrate with the following structures: ITO/NPB (50 nm)/CBP: 6% Dopant (30 nm)/BCP (10 nm)/AlQ_3 (30 nm)/LiF (1 nm)/Al. The organic and metal cathode layers were grown successively with a base pressure of $\sim 1 \times 10^{-6}$ Torr. In such a device, 4,4′-bis[*N*-(1-naphthyl)-*N*-phenyl-amino]biphenyl (NPB) acted as a hole transport layer, 2,9-Dimethyl-4,7-diphenyl-1,10-phenanthroline (BCP) as a hole blocking layer, tris-(8-hydroxyquinoline) aluminum(III) (AlQ_3) as an electron transport layer, 4,4′-bis(*N*-carbazolyl)biphenyl (CBP) as the host material, and iridium complexes as the dopant. The corresponding CIE coordinates are $x = 0.67$, $y = 0.33$ for $(\text{m-piq})_2$Ir(acac), $x = 0.70$, $y = 0.30$ for $(4\text{-pqz})_2$Ir(acac), $x = 0.70$, $y = 0.26$ for $(1\text{-mniq})_2$Ir(acac) and $x = 0.69$, $y = 0.30$ for $(2\text{-mniq})_2$Ir(acac) (as shown in Fig. 4). All four devices show red to deep-red emissions, following the same tendency that was observed in their PL spectrum data.

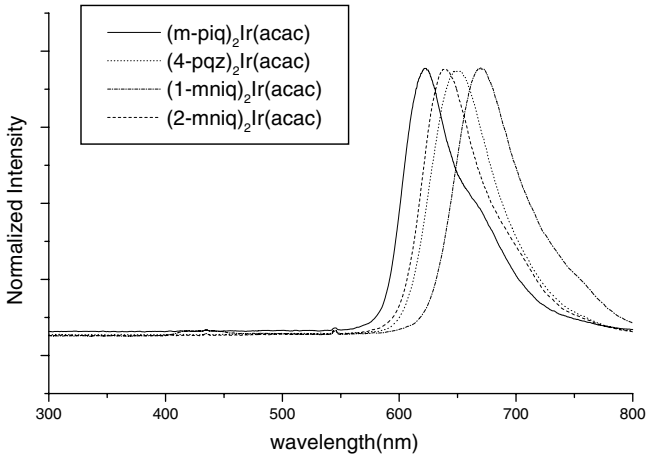

Fig. 2. EL spectra of iridium complexes.

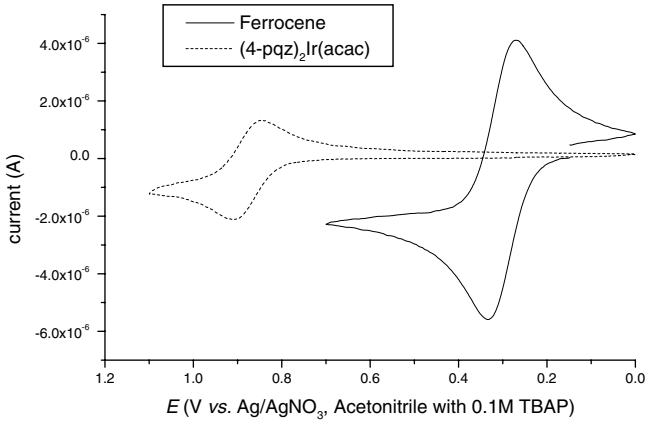

Fig. 3. The cyclic voltammogram of $(4\text{-pqz})_2$Ir(acac) at a Pt electrode. Scan rate: 50 mV/s, $T = 25$ °C.

Table 1
Electrophosphorescence, electrochemical data, HOMO, LUMO and energy gap data for iridium complexes

Compound	Brightness (cd/m^2)	LE (cd/A)	Current density (mA/cm^2)	Power efficiency (lm/W)	CIE coordinates	EL (nm)	$E_{1/2}$ (ox) (mV)[f]	HOMO (eV)	LUMO (eV)	Energy gap (eV)
$(m\text{-piq})_2Ir(acac)$	363[a]	9.84	3.7	5.15	$x = 0.67$	622.1	642 [341]	−5.14 (−4.76)[cal]	−3.11 (−1.77)[cal]	2.03 (2.99)[cal]
	941[b]	9.28	10.1	4.16	$y = 0.33$					
	2057[c]	8.69	23.7	3.41						
	4103[d]	8.27	49.6	2.88						
	8077[e]	8.17	98.9	2.56						
$(4\text{-pqz})_2Ir(acac)$	489[a]	3.14	15.6	1.64	$x = 0.70$	650.3	880 [579]	−5.38 (−5.10)[cal]	−3.46 (−2.22)[cal]	1.92 (2.89)[cal]
	1223[b]	3.02	40.6	1.35	$y = 0.30$					
	2570[c]	2.93	87.6	1.15						
	4893[d]	2.81	174.1	0.98						
	6800[e]	2.29	297.4	0.72						
$(1\text{-mniq})_2Ir(acac)$	9[a]	1.08	0.8	1.08	$x = 0.70$	669.5	615 [314]	−5.11 (−4.72)[cal]	−3.08 (−1.81)[cal]	2.03 (2.91)[cal]
	16[b]	0.55	2.9	0.55	$y = 0.26$					
	34[c]	0.43	7.9	0.43						
	73[d]	0.38	19.2	0.38						
	153[e]	0.36	42.4	0.36						
$(2\text{-mniq})_2Ir(acac)$	687[a]	1.83	19.6	1.83	$x = 0.69$	639.0	567 [266]	−5.07 (−4.64)[cal]	−3.04 (−1.90)[cal]	2.03 (2.74)[cal]
	1295[b]	1.47	39.6	1.47	$y = 0.30$					
	2192[c]	1.19	72.0	1.19						
	3505[d]	0.98	124.5	0.98						
	5128[e]	0.79	203.4	0.79						

For each parameter, the data in different rows correspond to those measured at different voltage: [a]: 6 V, [b]: 7 V, [c]: 8 V, [d]: 9 V, [e]: 10 V and [f]: $E_{1/2} = \frac{1}{2}(E_p^a + E_p^c)$ (vs. Ag^+/Ag), values in bracket are $E_{1/2}$ vs. ferrocene/ferrocenium. [Cal]Orbital energies calculated by density functional theory.

Electrophosphorescence data for the iridium complexes are summarized in Table 1. The data indicate that stronger bathochromic shifts (669.5 and 639.0, respectively) were observed when $(1\text{-mniq})_2Ir(acac)$ and $(2\text{-mniq})_2Ir(acac)$ were used as the dopant. This result implies that 1-(1′-naphthyl)-5-methylisoquinoline and 1-(2′-naphthyl)-5-methylisoquinoline exhibit different electronic transition dipole moments. This difference may disturbs the electron density of the iridium complex and reduces the band gap leading to the red shift effect. Because $(4\text{-pqz})_2Ir(acac)$ shows a bathchromic effect of about 10 nm in comparison with $(2\text{-mniq})_2Ir(acac)$, it is expected to result in poorer efficiency. Interestingly, $(4\text{-pqz})_2Ir(acac)$ shows almost the same emission characteristics in comparison with $(2\text{-mniq})_2Ir(acac)$. This result suggests that the electron density effect of the $(4\text{-pqz})_2Ir(acac)$ N(1) electronegative atom is equal to that of the extended π-conjugation effect of $(2\text{-mniq})_2Ir(acac)$, and the HOMO and LUMO values of $(4\text{-pqz})_2Ir(acac)$ apparently drop-off with the introduction of the nitrogen atom in N(1) in our data. As a result the energy gap of $(4\text{-pqz})_2Ir(acac)$ matches up with that of CBP and makes the hole transfer more efficient than with $(2\text{-mniq})_2Ir(acac)$, as shown in Fig. 5.

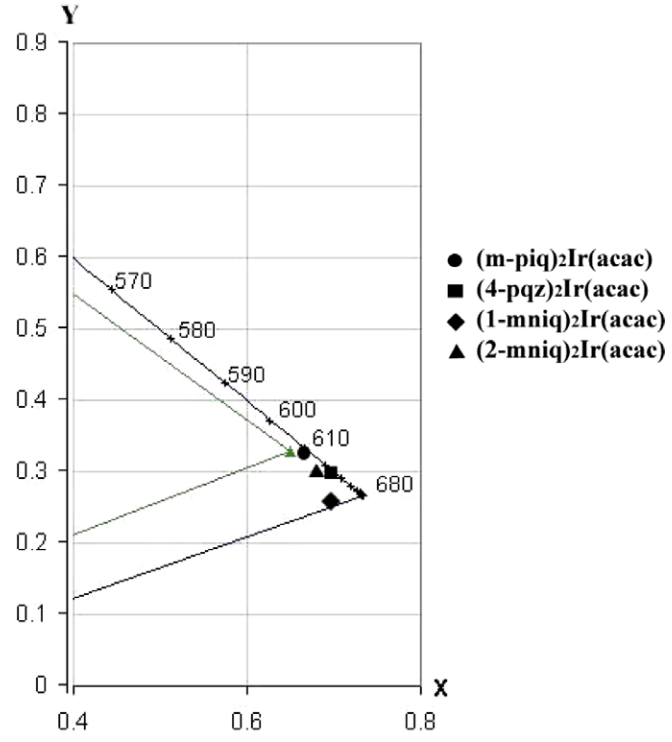

Fig. 4. CIE coordinates of $(m\text{-piq})_2Ir(acac)$ (0.67, 0.33), $(4\text{-pqz})_2Ir(acac)$ (0.70, 0.30), $(1\text{-mniq})_2Ir(acac)$ (0.70, 0.26) and $(2\text{-mniq})_2Ir(acac)$ (0.69, 0.30).

DFT calculations on four complexes were performed and contour plots of $(4\text{-pqz})_2Ir(acac)$ HOMO and LUMO are presented in Fig. 6 for illustration purpose. All of the $(\hat{C}N)_2Ir(acac)$ complexes that we have examined gave a similar courtier of plots of the HOMOs and LUMOs. As shown in Fig. 6, the HOMO (−5.38 eV) consists of a mixture of two phenyls, an iridium center, a part of the N(1) atom, and a part of the acetylacetonate orbitals while the LUMO (−3.46 eV) is predominantly on both 4-phenylquinazoline ligands. It is known from previous reports and our calculation results that the isoquinolyl ligands do not

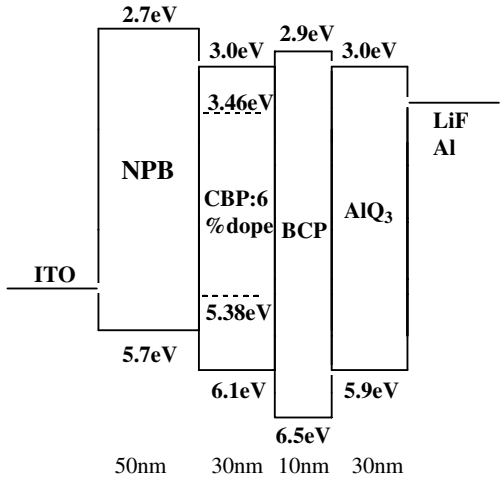

Fig. 5. Energy diagram of OLEDs using $(4\text{-pqz})_2\text{Ir(acac)}$ as dopant.

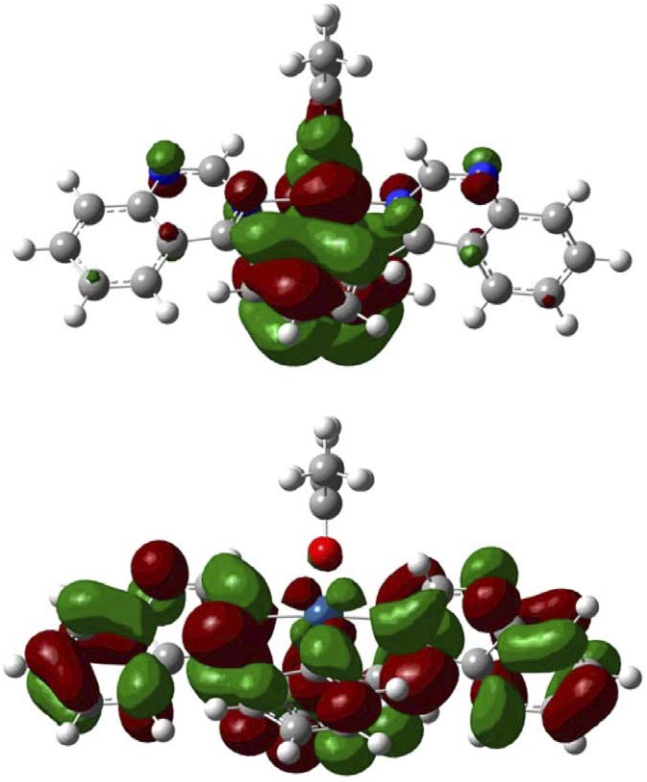

Fig. 6. HOMO (up) and LUMO (down) contour plots of $(4\text{-pqz})_2\text{Ir(acac)}$. (The figure shows that the HOMO of $(4\text{-pqz})_2\text{Ir(acac)}$ is virtually mixing of the iridium(III) 5d orbital with the π-system of two phenyl rings. However, LUMO is ligand-localized π^* orbitals of 4-phenyl quinazoline polarized to quinazoline rings).

contribute markedly to HOMO. However, Fig. 6 shows that the quinazolyl ligand N(1) atom does have some effects on HOMO. This result illustrated why the HOMO of $(4\text{-pqz})_2\text{Ir(acac)}$ was lower than $(\text{m-piq})_2\text{Ir(acac)}$. The contribution of Ir-d and two phenyl π-orbitals to the HOMO and the contribution of 4-phenylquinazolyl π^*-orbitals to LUMO were similar to those found in the related research [19,23].

Table 2
Comparison of T_1 energies calculated by TD-DFT with experimental EL data

Complexes	T_1 (eV) (cal.)	EL (eV) (exp.)
$(\text{m-piq})_2\text{Ir(acac)}$	2.05	1.99
$(4\text{-pqz})_2\text{Ir(acac)}$	2.00	1.91
$(1\text{-mniq})_2\text{Ir(acac)}$	1.88	1.85
$(2\text{-mniq})_2\text{Ir(acac)}$	1.95	1.94

It is apparent from Table 1 that when we introduce N(1) atom to the ligand, the CV and devices experimental data correspond to the calculation results. The calculated value of HOMO is close to the experiment value, however, the calculated LUMO does not agree well the experimental values due to the CH_2Cl_2 solvent effect.

The T_1 for each complex calculated by TD-DFT reveals a common characteristics arising from HOMO → LUMO dominant excitation, slows ^{3}MLCT transition. These results are compared with electroluminescence data and summarized in Table 2. The calculated T_1 energy of the iridium complexes agrees fairly well with experimental data. These results suggest an application of TD-DFT for predicting the emission of iridium complexes.

5. Conclusions

In summary, we have successfully designed and prepared 4-phenylquinazoline and phenyl-methylisoquinoline cyclometalated iridium complexes as new dopants for OLEDs, and estimated their HOMO, LUMO and band gap in DFT method using the Gaussian 98 suite of software. The results reveal a new direction in designing new ligands for light-emitting iridium complexes. We are preparing other isoquinoline and quinoline ligands with the N atom at different positions, and studying the behavior of the corresponding iridium complexes as dopants for OLEDs. The results will be reported in the near future.

Acknowledgements

This work was supported by the National Science Council of the Republic of China, Taiwan. (NSC 93-2113-M-006-019).

References

[1] M.A. Baldo, D.F. O'Brien, Y. You, A. Shoustikov, S. Sibley, M.E. Thompson, S.R. Forrest, Nature (London) 395 (1998) 151.
[2] L.S. Hung, C.H. Chen, Mater. Sci. Eng. R. 39 (2002) 143.
[3] S. Tokito, T. Lijima, T. Tsuzuki, F. Sato, Appl. Phys. Lett. 83 (2003) 2459.
[4] S. Lamansky, P. Djurovich, D. Murphy, F. Abdel-Razzaq, H. Lee, C. Adachi, P.E. Burrows, S.R. Forrest, M.E. Thompson, J. Am. Chem. Soc. 123 (2001) 4304.
[5] F. Chen, Y. Yang, M.E. Thompson, J. Kido, Appl. Phys. Lett. 80 (2002) 2308.
[6] C. Adachi, M.A. Baldo, S.R. Forrest, Appl. Phys. Lett. 78 (2001) 1662.

[7] W.S. Huang, J.T. Lin, C.H. Chien, Y.T. Tao, S.S. Sun, Y.S. Wen, Chem. Mater. 16 (2004) 2480.
[8] S. Okada, H. Iwawaki, M. Furugori, J. Kamatani, S. Igawa, T. Moriyama, S. Miura, A. Tsuboyama, T. Takiguchi, H. Mizutani, SID 02 DIGEST, 2002, p. 1360.
[9] C.H. Yang, C.C. Tai, I.W. Sun, J. Mater. Chem. 14 (2004) 947.
[10] T.Q. Chou, F.Y. Fu, Y.S. Kao, J. Am. Chem. Soc. 70 (1948) 1765.
[11] B.C. Uff, B.L. Joshi, J. Chem. Soc. Perkin Trans. 1 (1986) 2295.
[12] A.D. Becke, J. Chem. Phys. 98 (1993) 5648.
[13] C. Lee, W. Yang, R.G. Parr, Phys. Rev. B 37 (1988) 785.
[14] M.J. Frisch et al., Gaussian 98 Revision A.11, Gaussian, Inc., Pittsburgh, PA, 2001.
[15] P.J. Hay, W.R. Wadt, J. Chem. Phys. 82 (1985) 270.
[16] R.E. Stratmann, G.E. Scuseria, M.J. Frisch, J. Chem. Phys. 109 (1998) 8218.
[17] R. Bauernschmitt, R. Ahlrichs, Chem. Phys. Lett. 256 (1996) 454.
[18] M.E. Casida, C. Jamorski, K.C. Casida, D.R. Salahub, J. Chem. Phys. 108 (1998) 4439.
[19] P.J. Hay, J. Phys. Chem. A 106 (2002) 1634.
[20] M. Polson, S. Fracasso, V. Bertolasi, M. Ravaglia, F. Scandola, Inorg. Chem. 43 (2004) 1950.
[21] M.G. Colombo, A. Hauser, H.U. Gudel, Inorg. Chem. 32 (1993) 3088.
[22] (a) H.M. Koepp, H. Wendt, H. Strehlow, Z. Electrochem. 64 (1960) 483;
(b) P.E. Burrows, Z. Shen, V. Bulovic, D.M. McCarty, S.R. Forrest, J. Appl. Phys. 79 (1996) 7991.
[23] A.B. Tamayo, B.D. Alleyne, P.I. Djurovich, S. Lamansky, I. Tsyba, N.N. Ho, R. Bau, M.E. Thompson, J. Am. Chem. Soc. 125 (2003) 7377.